ChemComm

Accepted Manuscript

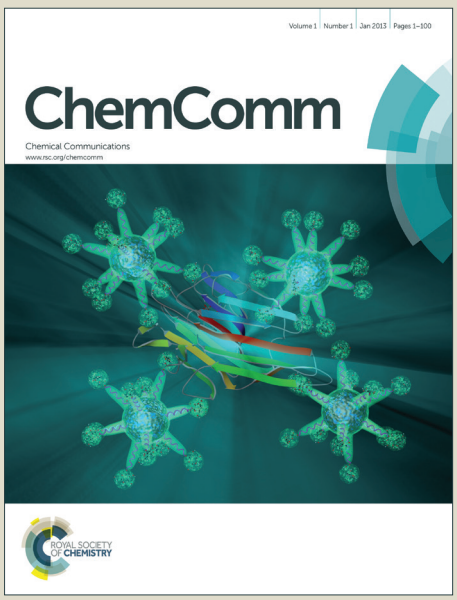

ROYAL SOCIETY OF CHEMISTRY

www.rsc.org/chemcomm

Cite this: DOI: 10.1039/c0xx00000x

www.rsc.org/xxxxxx

COMMUNICATION

Synergetic Plasmonic Effect of Al and Au Nanoparticles for Efficiency Enhancement of Air Processed Organic Photovoltaic Devices

George Kakavelakis[a,b], Emmanuel Stratakis[b,c] and Emmanuel Kymakis*[a]

Received (in XXX, XXX) Xth XXXXXXXXX 20XX, Accepted Xth XXXXXXXXX 20XX
DOI: 10.1039/b000000x

Enhancement in the efficiency of air processed bulk heterojunction photovoltaic devices is demonstrated via the addition of highly stable uncapped gold (Au) and aluminum (Al) nanoparticles (NPs) into the photoactive layer. An enhancement in conversion efficiency by 15% is observed, which can be attributed to Localised Surface Plasmon Resonance effects at the small diameter Au NPs and to efficient scattering by the large diameter Al NPs.

Bulk heterojunction (BHJ) organic photovoltaic (OPV) devices have many advantages, including low-cost, low-temperature fabrication, semi-transparency, and mechanical flexibility[1,2]. Rapid progress in the development of new polymers and device optimization has brought commercialization of OPV closer to reality, with recent reports of power conversion efficiencies (PCE) exceeding 10%[3,4]. However, the fundamental tradeoff between light absorption length and exciton diffusion length does not allow the increase of light absorption by simply using thicker BHJ films. The active layer is typically around 100 nm, whereas the exciton diffusion distances are 10 nm[5]. A thicker active layer offers higher light absorption, but, it comes at the expense of lowered charge collection. Therefore, it is essential to explore a device design, in which the thickness of the BHJ films will remain low, while the light absorption capability of the active layer will be maximized.

An effective way is the introduction of a light trapping mechanism, enabling to thin down the OPV device without sacrificing efficiency, leading to lower material utilization and a cost benefit[6]. Lately, metallic nanoparticles (NPs) of various sizes, shapes and configurations have been integrated into the OPV cell architecture (inside photoactive[7,8,9,10], or buffer layer[11,12,13], or between interfaces[14,15,16]) in order to enhance, in a wavelength-dependent manner, the optical absorption of the respective devices. Metallic NPs are known to exhibit a strong absorption band in the UV–visible region, which lies within the optical absorption band of the conjugated polymers used in the active layer OPVs. Small NPs with diameters in the range 5-20 nm behave as subwavelength antennas, due to excitation of localized surface plasmon resonance (LSPR). On the other hand, relatively larger diameter NPs behave as effective subwavelength scattering elements that couple and trap freely propagating plane waves of the incident light into the photoactive layer. Alternatively, NPs can be placed in the form of a periodically arranged nanoarray at the front or back contact of OPV devices. In this case, incident light scattered by such nanoarray is coupled into waveguide modes coined as surface plasmon polaritons (SPP)[17].

The incorporation of metallic NPs into the photoactive layer has proven to be the most successful way of enhancing efficiency, either via the formation of scattered waves at the large diameter NPs[18] or due to excitation of LSPR modes at the smaller diameter NPs[19]. Nevertheless, the utilization of chemically synthesized NPs is problematic, since the presence of surfactants and ligand coatings promotes undesirable exciton quenching, via nonradiative energy transfer between the NPs and the active layer, which decreases the plasmonic improvement effect[20]. In this context, metallic NPs synthesized by ablation in liquids with pico- and femtosecond laser pulses which are free of surfactants and ligand layers[21], are ideal for use as additives. Au and Al NPs were recently successfully utilized as additives in the active layer of poly(3-hexylthiophene) (P3HT) -[6,6]-phenyl-C61-butyric acid methyl ester (PCBM) OPVs leading to both efficiency and stability enhancement by our group. In particular, the addition of Au NPs into the active layer enhances the performance of a typical device by 40% compared to a pristine device due to LSPR[22]. While, the incorporation of Al NPs into the active layer enhances the OPV performance by 30% compared to the pristine device due to scattering effects[23]. In both cases, the dispersion of NPs into the photoactive layer also leads to an improvement of its structural stability, since the NPs act as quenchers of the triplet excitons and in this way the photo-oxidation process is impeded [24,25].

In this work, the performance of OPV devices is enhanced by a synergetic effect of both LSPR and scattering. In particular, small diameter Au NPs, as well as large diameter Al NPs are dispersed into the photoactive layer in order to contribute to optical absorption enhancement by plasmonic and scattering effects respectively. In addition the poly[N-9-hepta-decanyl-2,7-carbazolealt-5,5-(4,7-di-2-thienyl-2,1,3-benzothiadiazole)] (PCDTBT) is chosen as the electron donor material instead of the air sensitive P3HT.

As prepared Al and Au NPs were spherical and had relatively uniform diameters. The respective size distribution determined from a series of TEM images (Fig. S1) is presented in Fig.S2. Fig. 1a shows the transmission electron microscopy (TEM) image of the Au-Al mixture of NPs used as additive in this work. While, Fig. S1 shows the TEM images of the individual Au and Al NPs. The analysis of the TEM images indicate that the majority of Al NPs exhibit sizes ranged from 10 to 70 nm with an average of ~30 nm and the majority of Au NPs exhibit sizes ranged from 1.5 to 20 nm with an average of ~10nm, as shown also in the histograms in Fig.S2.

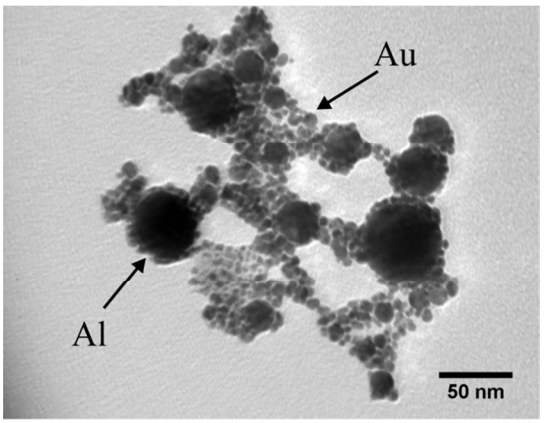

Fig. 1 TEM images of the fabricated dual Al and Au NPs solution

The corresponding absorption spectra of the colloidal Al, Au and dual Al-Au NPs solutions in ethanol are shown in Fig.S3. The Au NPs exhibit a distinct peak at 535 nm, which correspond to the theoretically predicted enhanced absorption due to plasmon resonance. On the contrary, the Al NPs colloid exhibits strong absorption in UV, while the absorption edge protrudes to the visible region. As expected, the absorption of dual NPs solution is a superposition of the two individual spectra. Fig. S4 shows the UV-Vis absorption spectra of pristine, Au doped, Al doped and Al-Au doped PCDTBT-$PC_{71}BM$ blends. Fig. S5 presents the absorption enhancement curves calculated for the respective blends (ratios of the absorption spectra of the NPs based devices to that of the pristine one). It is clear that dual NPs shows superior absorption enhancement compared with single ones. Furthermore, the characteristic peak in the absorption enhancement curve of the Au-doped device is close to the calculated extinction spectrum of the Au NPs embedded in the PCDTBT-$PC_{71}BM$ medium[26]. On the contrary, in Al doped device the absorption improvement is constant within the entire wavelength range. Considering that the LSPR of Al NPs lies in the UV region, the observed enhancement can be attributed to light scattering from Al NPs. Finally, in the dual doped device, the synergetic effect of both types of NPs can be observed. Indeed, the absorption increase is roughly the sum of the two individual enhancements, suggesting that both NP types may equally contribute to the enhanced absorption.

Fig. 2 shows the current density-voltage (J-V) curves of the pristine and OPV devices doped with Au, Al, Au-Al NPs, under illumination with 100 mW/cm^2 light intensity.

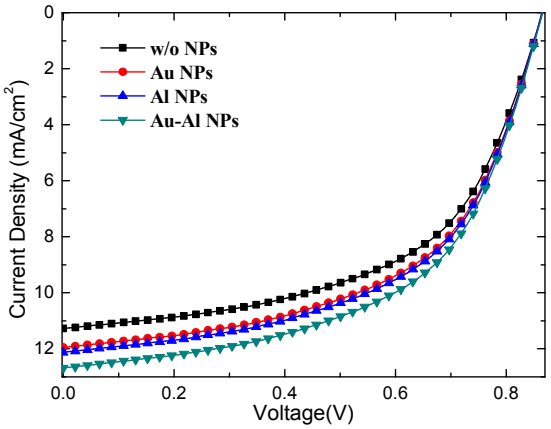

Fig.2 J-V characteristics of the OPV devices with Al NPs, Au NPs and dual Au and Al NPs embedded in the active layer.

The respective averaged photovoltaic characteristics are summarized in Table I.

Table I: Photovoltaic performance comparison of the devices

NPs	J_{SC} (mA/cm^2)	V_{OC}(V)	FF (%)	PCE (%)
No	11.27 ± 0.12	0.86	55.00± 0.30	5.33± 0.05
Au	11.95± 0.20	0.86	56.00± 0.40	5.76± 0.09
Al	12.12± 0.24	0.86	56.00± 0.54	5.84± 0.12
Au-Al	12.71± 0.15	0.86	56.00± 0.48	6.12± 0.08

In particular, it is observed that the incorporation of Au NPs in the active layer induces an enhancement of 6% to the short-circuit current (J_{SC}), whereas the open-circuit voltage (V_{OC}) remains constant and the fill factor showed an enhancement of 2%. Incorporation of Al NPs gives rise to an enhancement of 8% to J_{SC}, whereas V_{OC} remains constant and FF is enhanced by 2%. On the other hand, the dual NPs device exhibits a power conversion efficiency of 6.12%. From the photovoltaic and the absorption enhancement results, we can conclude that a synergetic effect of Al and Au NPs takes place, which leads to an overall efficiency enhancement of 14.8% compared to undoped cells. Another point to be noted is that the efficiency enhancement upon NPs doping is directly related to the structural stability of the OPV device, since all the fabrication process takes place in ambient conditions. In the case of Au doped P3HT:PCBM devices, an efficiency enhancement of 40% is observed, leading to an efficiency of 3.71%. In the PCDTBT:$PC_{71}BM$ system, which is much more stable against oxygen and humidity[27], an efficiency enhancement of 14.8% is observed, with a much higher efficiency of 6.12%. Therefore, it is more than obvious, that the NPs block the photo-oxidation process in OPVs, in full agreement with our previous studies[24].

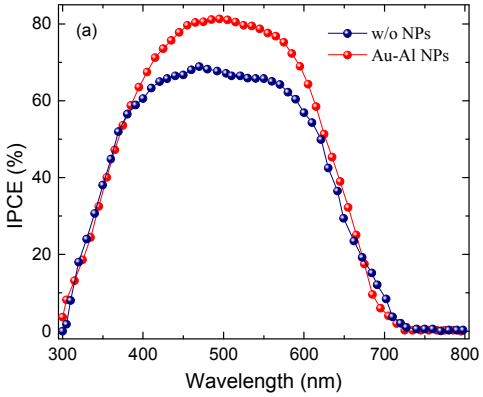

Fig.3 a) IPCE curves of the OPV devices b) Comparison between the curve of the increase in IPCE (DIPCE) after incorporating dual NPs

In order to get an insight for the responsible mechanism to the enhanced performance of the devices, the incident photon-to-electron conversion efficiency (IPCE) curve of the dual NPs device is measured and compared with that of the pristine one(Fig.3a). The corresponding increase in IPCE (ΔIPCE) after incorporating dual NPs is also presented in Fig.3b. The pristine device exhibits a maximum IPCE of ~69%, while the dual doped device exhibits an enhanced maximum of ~81%. As shown in Fig.3b, the IPCE enhancement is broad and almost uniform ranging from 450 to 600 nm, which can be directly attributed to multiple scattering effects by the large diameter Al NPs[28]. Therefore, the IPCE enhancement follows the increase in the optical absorption, indicating that a synergetic effect of LSPR and scattering from the Au and Al NPs respectively takes place. This is in contrast to the case of the P3HT:PCBM system, in which a disparity between the absorption and IPCE enhancement was observed, indicating the existence of an additional enhancement mechanism, such as the improvement of the photoactive layer morphology[22]. It should be also noted that the integrated J_{sc} values from the IPCE spectrum for the pristine and the dual NPs devices are 10.94 and 12.37 mA/cm^2, respectively, which are only ~3% different than the actual measured J_{SC} values, indicating good accuracy of the OPV measurement.

In order to further support that the IPCE enhancement in the 400-600 nm is due to multiple scattering effects, the diffuse reflectance of the devices was recorded and presented in Fig. S6. In this region, the lower reflectivity of the devices doped with NPs, clearly indicates stronger absorption due to scattering. The scattering effect of Al NPs increases the effective length of the optical path, which in turn increases the generation of electron–hole pairs. Furthermore, the lower reflectivity observed in the Au doped device indicating that the formation of Au NPs clusters may be possible.

To summarize, we demonstrated highly efficient air processed plasmonic OPVs that incorporate a mixture of Au and Al NPs into the PCDTBT:$PC_{71}BM$ photoactive layer. The PCE measured to be 6.12%, enhanced to by ~15% with respect to the undoped device. The efficiency enhancement attributed to improved absorption caused by a synergy of LSPR and scattering effects.

Acknowledgements

The authors acknowledge M. Androulidaki for her support with the IPCE experiments.

Notes and references

[a] *Center of Materials Technology and Photonics & Electrical Engineering Department, School of Applied Technology, Technological Educational Institute (TEI) of Crete, Heraklion, 71004, Crete, Greece. E-mail: kymakis@staff.teicrete.gr; Tel:+30-2810379895*

[b] *Dept. of Materials Science and Technology, Univ. of Crete, Heraklion, 71110 Crete, Greece*

[c] *Institute of Electronic Structure and Laser (IESL), Foundation for Research and Technology-Hellas (FORTH) Heraklion, 71110 Crete, Greece.*

† Electronic Supplementary Information (ESI) available: [TEM images, size distribution and UV-VIS spectra of the fabricated Au and Al NPs. Absorption spectra and absorption enhancement factors of the BHJ devices with Al NPs, Au NPs and dual NPs embedded in the active layer. Reflectance spectra of the respetive devices fabricated]. See DOI: 10.1039/b000000x/

[1] S. H. Park, A. Roy, S. Beaupré, S. Cho, N. Coates, J. S. Moon, D. Moses, M. Leclerc, K. Lee, A. J. Heeger, *Nat. Photonics* 2009, **3**,297-303
[2] H. Y. Chen, J. H. Hou, S. Q. Zhang, Y. Y. Liang, G. W. Yang, Y. Yang, L. P. Yu, Y. Wu, G. Li, *Nat. Photonics* 2009, **3**, 649-653
[3] J. You, L. Dou, K. Yoshimura, T. Kato, K. Ohya, T. Moriarty, K. Emery, C. Chen, J. Gao, G. Li and Y. Yang, *Nat. Communications*, 2013, **4**, 1446
[4] Z. He, C. Zhong, S. Su, M. Xu, H. Wu, Y. Cao, *Nat. Photonics*, 2012, **6**, pp. 591–595
[5] G. Dennler, M. C. Scharber and C. J. Brabec, *Adv. Mater*., 2009, **21**, 1323–1338.
[6] E.T. Yu, J. Van De Lagemaat, *MRS Bulletin*, 2011, **36**, 424-428.
[7] C. H. Kim , S.H. Cha , S.C. Kim , M. Song , J. Lee , W.S. Shin , S.J. Moon , J.H. Bahng , N.A. Kotov , S.H. Jin , *ACS Nano* 2011, **5**, 3319-3325
[8] X. Li , W.C.H. Choy, H. Lu , W.E.I. Sha , A.H.P. Ho, *Adv. Funct. Mater*. 2013, **23**, 2728–2735
[9] D. H. Wang, K. H. Park, J. H. Seo, J. Seifter, J. H. Jeon, J. K. Kim, J. H. Park, O. O. Park, A. J. Heeger, *Adv. Energy Mater*. 2011, **1**, 766–770
[10] B.Paci, G.D. Spyropoulos , A. Generosi , D. Bailo , V. R. Albertini , E. Stratakis , E. Kymakis, *Adv. Funct. Mater*. 2011, **21**, 3573–3582
[11] Y.S. Hsiao , S. Charan , F.Y. Wu , F.C. Chien , C.W. Chu , P. Chen , and F.C. Chen, *J. Phys. Chem. C,* 2012, **116**, 20731.
[12] D.D.S. Fung, L. Qiao, W.C.H. Choy, C.C.D. Wang, W.E.I. Sha, F. Xie, S. He, *J. Mater. Chem* 2011, **21**,16349 - 16356,
[13] L. Lu, Z. Luo, T. Xu, L. Yu, *Nano Letters* 2013, 13,59-64
[14] E. Stratakis, M.M. Stylianakis, E. Koudoumas, E. Kymakis, *Nanoscale*, 2013, **5** , 4144-4150
[15] S. Shahin, P. Gangopadhyay, R. A. Norwood, *Appl. Phys. Lett.,* 2012, **101**, 053109
[16] E. Kymakis, E. Stratakis, E. Koudoumas, C. Fotakis, *Photonics Nanostruct.,* 2011, **9**, 184–189.
[17] E. Stratakis, E. Kymakis , *MaterToday*, 2013, **16**, 138-151
[18] D. H. Wang, D. Y. Kim, K. W. Choi, J. H. Seo, S. H. Im, J. H. Park, O. O. Park, and A. J. Heeger,Angew. Chem. Int. Ed.2011, 50, 5519 –5523
[19] J.-Y. Lee, P. Peumans, *Optics Express*, 2010 **18**, 10078.
[20] K. Topp, H. Borchert, F. Johnen, A. V. Tunc, M. Knipper, E. von Hauff, J. Parisi, *K*. Al-Shamery, *J Phys Chem A,* 2010, **114**, 3981.
[21] E. Stratakis, M. Barberoglou, C. Fotakis, G. Viau, C. Garcia, G.A. Shafeev, *Opt. Express*, 2009, **17**, 12650
[22] G.D. Spyropoulos, M.M. Stylianakis, E. Stratakis, E. Kymakis, *Appl. Phys. Lett*., 2012,**100**, 213904
[23] G. Kakavelakis, E. Stratakis, E. Kymakis, *RSC Adv.*, 2013,**3**, 16288-16291
[24] B. Paci, A. Generosi, V.R. Albertini, G.D. Spyropoulos, E. Stratakis , E. Kymakis, *Nanoscale*, 2012, **4**, 7452–7459
[25] B. Paci, D. B., Bailo V. D., Albertini, J. V., Wright, C. J., Ferrero, G.D. C., Spyropoulos, E. G.D., Stratakis, E. E.,Kymakis, E, , *Adv. anced Mater.ials,* 2013, **25**(34), 4760–4765.
[26] G. on Namkoong, J. aemin Kong, M. atthew Samson, I.W. In-Wook Hwang, Kwanghee K. Lee, *Organic Electronics,* 2013, **14** 74–79
[27] D. H. Wang, J. K. Kim, J. H. Seo, O. O. Park, J. H. Park, *Sol Ener Mat Sol Cells* 2012, **101**, 249–255
[28] S.W. Baek, J. Noh, C.H. Lee, B.S. Kim, M.K. Seo and J.Y. Lee, *Scientific Reports*, 2013, **3,** 1726